

Assessment of mass-transfer effects and elementary reaction scheme for catalytic reactors

P. Praveen Kumar

A Thesis Submitted to
Indian Institute of Technology Hyderabad
In Partial Fulfillment of the Requirements for
The Degree of Master of Technology



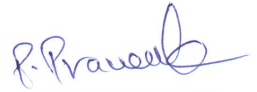
भारतीय प्रौद्योगिकी संस्थान हैदराबाद
Indian Institute of Technology
Hyderabad

Department of Chemical Engineering

September 2011

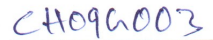
Declaration

I declare that this written submission represents my ideas in my own words, and where ideas or words of others have been included, I have adequately cited and referenced the original sources. I also declare that I have adhered to all principles of academic honesty and integrity and have not misrepresented or fabricated or falsified any idea/data/fact/source in my submission. I understand that any violation of the above will be a cause for disciplinary action by the Institute and can also evoke penal action from the sources that have thus not been properly cited, or from whom proper permission has not been taken when needed.



(Signature)

(P. Praveen Kumar)



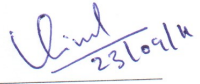
(Roll No.)

Approval Sheet

This Thesis entitled **Assessment of mass-transfer effects and elementary reaction scheme for catalytic reactors** by **P. Praveen Kumar** is approved for the degree of Master of Technology from IIT Hyderabad



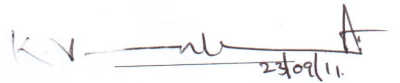
(Dr. Raja Benerjee) Examiner
Department of Mechanical Engineering
IIT Hyderabad



(Dr. Vinod M. Janardhanan) Adviser
Department of Chemical Engineering
IIT Hyderabad



(Dr. Saptarshi Majumdar) Examiner
Department of Chemical Engineering
IIT Hyderabad



(Dr. K. Venkatasubbaiah) Chairman
Department of Mechanical Engineering
IIT Hyderabad

Acknowledgements

This theses would not have been possible without the guidance and the help of several individuals who contributed and extended their valuable assistance in the preparation and completion of this study.

First and foremost, my utmost gratitude to Dr. Vinod M. Janardhanan, my thesis advisor whose sincerity and encouragement I will never forget. He has been my inspiration as I hurdle all the obstacles in the completion of this thesis work. The supervision and support that he gave truly helped the progression and smoothness of my master's program.

I am thankful to our Director Prof. U. B. Desai for providing us with an environment to complete our project successfully.

I am deeply indebted to then Head of the Department Prof. Srinivas jayanti, who inspired me excel technically.

I would like to thank all the faculty members of department of Chemical Engineering, IIT Hyderabad for their constant encouragement.

I am ever grateful to my institute, IIT Hyderabad for providing the necessary infrastructure and financial support. I thank the office staff of IIT Hyderabad for their prompt and generous help. I would also like to thank the computer lab, IIT Hyderabad for providing excellent computation facilities.

I would like to thank my M.Tech, PhD colleagues and Friends for their constant support.

Finally I thank my parents for their encouragement and support for my ideas and decisions.

To my parents

Nomenclature

z	:	Horizontal coordinate
r	:	Radial coordinate
u	:	Horizontal velocity
P	:	Perimeter of the channel
ρ	:	Density of the fluid mixture
Y_i	:	Mole Fraction of component i
A_c	:	Cross sectional Area
d	:	Diameter of the channel
$\dot{\omega}_i$:	Molar production of gasphase component i
\dot{s}_i	:	Molar production of surface species i
p	:	Pressure in Pa
M_{avg}	:	Average molecular weight of the mixture
T_b	:	Temperature of the bulk fluid
Re	:	Reynolds number
R_g	:	Universal Gas constant
Pr	:	Prandtl number
$k_{m,i}$:	Mass transfer coefficient of species i
$Y_{i,s}$:	Mole fraction of the species i at the surface
j_i	:	Radial diffusion flux
D_i	:	Diffusivity of species i
Nu	:	Nusselt number
Gz	:	Graetz number
μ	:	viscosity
Sh	:	Sherwood number
Sc	:	Schmidt number
k_f	:	Forward rate constant
k_r	:	Reverse reaction rate coefficient

Abstract

Catalytic combustion is carried out in a tubular reactor of radius in the order of millimeters and a length of around 10 centimeters in presence of catalysts Rhodium and Platinum. For mass transfer coefficient calculation in the modeling of mass transfer between the bulk of the fluid to the surface, correlations developed by Tronconi and Forzatti(1992) are used. The results shows that the assumption stating both the bulk concentration and concentration at the surface are same, deviates from the actual scenario. The combustion is actually slow than what PFR predicts when we observed the mass transfer limited catalytic combustion. A discrepancy is observed with the mechanism of methane partial combustion in the presence of Rhodium catalyst in terms of the concentrations of CO_2 and H_2O mole fractions, the mechanism gives more CO_2 and H_2O than the equilibrium composition.

Contents

Declaration	ii
Approval Sheet	iii
Acknowledgements	iv
Nomenclature	vi
Abstract	vii
1 Introduction	1
1.1 Background	1
2 Modeling of Tubular Reactors	3
2.1 Governing equations of PFR	3
2.2 Modeling of PFR with mass and heat transfer limitations	4
2.3 2-D Modeling of tubular catalytic reactor	4
2.4 Boundary Condition	6
2.5 Transport Properties	6
2.5.1 Pure species viscosity and Binary diffusion coefficients	6
2.5.2 Pure species Thermal Conductivity	8
2.5.3 Mixture Average Properties	9
2.6 Thermodynamic Properties	10
2.7 Mixture average properties	11
2.8 Results and Discussions	12
2.9 Summary	16
3 Equilibrium Composition Calculations	17
3.1 Formulation	17
3.2 Results and Validation	19
3.3 Summary	20
4 Mechanism Validation	21
4.1 Background	21
4.2 Results and Discussions	22
4.3 Summary	26
5 Summary	27
References	28

Chapter 1

Introduction

1.1 Background

These are the days the world is obsessed with energy, its efficient utilization and environment pollution control. Combustion is the major way of extracting energy to put it into many useful forms from various fuels available in different forms. So combustion is inevitable process in today's world, which is also one of the major source of green house and hazardous gases in the atmosphere. Exhaust gases from industrial processes are sources of hazardous gases like CO, NO, NO₂, sulfur oxides present in the environment. Hence developing efficient combustion technologies will ensure effective utilization of fuel resources and also reduce the harmful gases in the exhausts. This gives a strong motivation for the current study.

Combustion can be two types namely homogeneous combustion also called as conventional combustion and catalytic combustion. It is appropriate to have some understanding of these two types of combustion. Majority of the differences are[1]

- 1) Conventional combustion happens in presence of a flame, where as catalytic combustion is a flameless process.
- 2) Catalytic combustion is a low temperature process when compared to conventional combustion.
- 3) Catalytic combustion releases very less oxides of Nitrogen
- 4) Conventional combustion can be realized only in a certain limit of fuel to oxygen ratio known as flammability limit, whereas catalytic combustion is not so dependent on fuel to air ratio.
- 5) Less constraints on reactor design with catalytic combustion.

Conventional combustion happens at certain compositions of fuel in air, which is known as the flammability limit. It depends on the fuel, each fuel will have a different flammability limit. For methane it is 5% to 16% of methane by volume. A spark or a pilot flame is required to initiate the combustion in conventional combustion. Usually too much of air or inert gas will be sent to lower the temperatures in conventional combustion. Conventional combustion occurs in a chamber called firebox or furnace. Sufficient space should be allowed to develop the flame and to avoid impingement of the flame on the wall. So large chambers are required for conventional combustion and due to high combustion temperatures there is a problem of NO_x formation. Catalytic combustion doesn't require any spark or pilot flame, it doesn't form flame, has no flammability limits, but a minimum gas inlet temperature is necessary to achieve maximum catalytic activity. The temperatures in the

catalytic combustor are much lesser than conventional combustion at which thermal NO_X formation is very less and flame impingement is not a problem.

Therefore catalytic combustion promises a cleaner combustion process, and makes the design of combustion furnaces and reactors more compact. Low calorific value fuels can be utilized for combustion in catalytic combustors, where as it is difficult to sustain the flame in conventional combustion. Catalytic combustors are also used to combust volatile organic compounds(VOC) at low concentrations in air streams. Low temperature combustion in catalytic combustors offers low formation of NO_X and they can also be used to combust exhausts from vehicles which contain carbon monoxide, hydrocarbon and NO_X , are known as catalytic converters. This gives an idea how important is catalytic combustion for various combustion applications which is cleaner in the emissions unlike conventional combustion processes. Early observation of study on catalytic combustion can be seen with the research of Sir Humphrey Davy(1818), who had devised a safety lamp to use in the underground coal mines using a platinum wire with air and coal gas to make the wire hot without a flame, which is required as there will be methane gas in the underground coal mines which may cause fire accidents.

Catalytic combustion can be operated in two ways 1) Catalytic combustion, 2) Catalytically supported homogeneous combustion. In the first case the combustion reactions occur on the surface of the catalyst surface. In the second case reactions on catalyst surface generate intermediate species and this process will also increase the temperature of the bulk fluid, which is sufficient to carry out the gas phase combustion and sustain the homogeneous gas phase reactions[1]. In the first case motivation is to reduce gas phase reactions and in the second case to initiate the gas phase reactions. The catalyst will be different in these two cases.

Monolithic reactors are being used in many combustion applications for heat generation, and eliminating NO_X ,CO from the exhaust gases. Heat generation case applies to gas turbines with catalytic combustor systems[2]. Major applications of monoliths are in the pollution abatement from stationary and non-stationary sources, such as treatment of exhaust gases from cars, decomposition of ozone in aircrafts, reduction of NO_X , destruction of volatile organic compounds(VOC), and in catalytic combustion applications.

Monoliths involve combination of single reactor such as circular or tubular, square, etc. Current study is carried out to understand the modeling of catalytic tubular reactors by incorporating the mass and heat transfer effects. Tubular reactors are also used in other various processes. Apart from the above applications, some are in hydrogenation and dehydrogenation, hydrocracking, oxidative decomposition, reforming[3].

Here mass transfer effects, combustion mechanism validation and order prediction of the combustion reactions are carried out. Major challenge in carrying these simulations is getting the solutions stabilized or getting a convergent solution. A study to compare the plug flow reactors, with boundary layer model and Navier-Stokes models. Where both boundary layer model and Navier-Stokes model are 2D[4], we are studying the behaviour of a 1D model when mass transfer coefficients are used to model the mass transfer and we are comparing with a 2D boundary layer model.

Chapter 2

Modeling of Tubular Reactors

Modeling of tubular reactors can have various levels of complexity based on number of mass and heat transfer effects included in the system. Tubular catalytic reactor can be modeled by considering the concentration and temperature of the bulk fluid and the solid wall as same, and is known as pseudo-homogeneous model, and by modeling bulk fluid and solid wall separately connecting through transport equations for mass and heat transfer, the model is known as heterogeneous model. Ideal plug flow reactors are modeled as one dimensional in the axial direction and considering same temperature and concentration at the wall and in the fluid.

2.1 Governing equations of PFR

A 1D steady state plug flow reactor is considered, with uniform temperature and concentration in the bulk fluid as well as at the wall. Fig.(2.1) is a schematic representation of the elemental volume considered for the mass and energy balance equations.

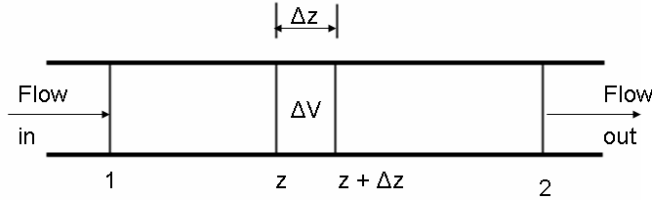


Figure 2.1: Representation of 1D Plug flow reactor, with a control volume of ΔV and of length Δz

$$\frac{d}{dz}(\rho u) = 0, \quad (2.1)$$

$$\frac{d}{dz}(\rho u Y_i) = \dot{\omega}_i W_i + \frac{4}{d} \dot{s}_i W_i, \quad (2.2)$$

$$\rho u A_c \frac{d}{dz} (C_p T_b) = -(\Sigma \dot{\omega}_i h_i M_i A_c + \Sigma \dot{s}_i h_i M_i P) + hP(T_w - T_b), \quad (2.3)$$

$$p M_{avg} = \rho R_g T_b \quad (2.4)$$

These equations describe the mass balance, species balance, energy balance and ideal gas equations respectively. Where T_b is the bulk temperature of the fluid, T_w is the wall temperature, $\dot{\omega}_i$, \dot{s}_i are the molar production rates of species i due to gas phase reaction and surface reaction.

2.2 Modeling of PFR with mass and heat transfer limitations

Mass transfer to the wall due to convection from the fluid and the mass transfer due to diffusion in the axial direction need to be incorporated in order to study the effect of mass transfer phenomena on the system. Considering $k_{m,i}$ as mass transfer coefficient and $D_{i,A}$ diffusion coefficient is used. Below are the governing equations with axial diffusion, convective mass transfer to the wall and heat transfer from wall.

$$\frac{d}{dz}(\rho u) = 0 \quad (2.5)$$

$$\frac{d}{dz}(\rho u Y_i) = \dot{\omega}_i M_i + \frac{4}{d} \dot{s}_i M_i \quad (2.6)$$

$$k_{m,i} \rho (Y_i - Y_{i,s}) = \dot{s}_i M_i \quad (2.7)$$

$$\rho u A_c \frac{d}{dz} (C_p T_b) = -(\Sigma \dot{\omega}_i h_i M_i A_c + \Sigma \dot{s}_i h_i M_i P) + hP(T_w - T_b), \quad (2.8)$$

$$p M_{avg} = \rho R_g T_b \quad (2.9)$$

2.3 2-D Modeling of tubular catalytic reactor

It is based on the boundary layer approximation, it is applicable for systems with a main direction of the convective flow, in which diffusive transport along this direction is negligible compared to convection. This assumption is valid for any cylindrical reactor with sufficiently high velocity of the fluid or very sufficiently small diameter of the channel. All the other transport effects within the fluid, diffusion limitations of surface reaction rates, are considered in this approximation. Governing equations are[5]

$$\frac{\partial(r\rho u)}{\partial z} + \frac{\partial(r\rho v)}{\partial r} = 0 \quad (2.10)$$

$$\frac{\partial(r\rho u^2)}{\partial z} + \frac{\partial r\rho uv}{\partial r} = -r \frac{\partial p}{\partial z} + \frac{\partial}{\partial r} \left(\mu r \frac{\partial u}{\partial r} \right) \quad (2.11)$$

$$\frac{\partial p}{\partial r} = 0 \quad (2.12)$$

$$\frac{\partial(r\rho uh)}{\partial z} + \frac{\partial(r\rho vh)}{\partial r} = u \frac{\partial p}{\partial z} + \frac{\partial}{\partial r} \left(\lambda r \frac{\partial T}{\partial r} \right) - \frac{\partial}{\partial r} \left(\sum_i r j_i h_i \right) \quad (2.13)$$

$$\frac{\partial(r\rho u Y_i)}{\partial z} + \frac{\partial(r\rho v Y_i)}{\partial r} = -\frac{\partial}{\partial r} (r j_i) + r \dot{\omega}_i \quad (2.14)$$

Above equations represent the total continuity, axial momentum, radial momentum, energy and species continuity respectively. The flux j_i is calculated as

$$j_i = \left\{ \begin{array}{lll} \dot{s}_i & \text{if} & r = r_{min} \\ -\rho D_i \frac{M_i}{M} \frac{\partial X_i}{\partial r} & \text{if} & r_{min} < r < r_{max} \\ -\dot{s}_i & \text{if} & r = r_{max} \end{array} \right\} \quad (2.15)$$

Where v is the radial velocity, r is the radial coordinate, h is enthalpy density of reacting mixture, h_i is the species enthalpy, j_i is the radial diffusion flux. The coupled equations are solved using implicit code LIMEX in *DETCHEM^{CHANNEL}*.

The above Eq. 2.6 and 2.7 include the mass transfer($k_{m,i}$) due to convection and molecular diffusion(D) in the axial direction. Solving these equations requires the knowledge of h and $k_{m,i}$ values as a function of axial position, as these values vary with temperature, velocity, viscosity and with axial position. For the case of simultaneous boundary layer development the correlation developed by Tronconi and Forzatti(1992) are used. The equations for constant wall temperature are

$$Nu_T = 3.656 + 8.827 \left(\frac{1000}{Gz} \right)^{-0.545} \exp \left(\frac{-48.2}{Gz} \right) \quad (2.16)$$

For constant wall heat flux the below equation gives local heat transfer coefficient.

$$Nu_H = 4.364 + 13.18 \left(\frac{1000}{Gz} \right)^{-0.524} \exp \left(\frac{-60.2}{Gz} \right) \quad (2.17)$$

Here Nu_T , Nu_H are Nusselt number for constant wall temperature and for constant wall heat flux respectively. Nusselt number is defined as follows

$$Nu = \frac{hL}{k_f} \quad (2.18)$$

Here h is the convective heat transfer coefficient of the fluid, L is the characteristic length (D_T in this tubular reactor case), k_f is thermal conductivity of the fluid. Graetz number Gz is defined as below

$$Gz = \frac{D_T}{z} Re Pr \quad (2.19)$$

Where Re is Reynolds number defined based on the tube diameter D_T as below

$$Re = \frac{D_T u \rho}{\mu} \quad (2.20)$$

and Pr is Prandtl number defined based on the fluid properties as below

$$Pr = \frac{C_p \mu}{k_f} \quad (2.21)$$

where C_p , μ , k_f are specific heat, viscosity, conductivity of fluid respectively. For finding the local mass transfer coefficient we will use the Sherwood number calculated as below for the two different cases of constant wall temperature(Eq. 2.16) and constant wall heat flux(Eq. 2.17) for the case of simultaneous development of thermal and hydrodynamic boundary layer situation.

$$Sh_T = 3.656 + 8.827 \left(\frac{1000}{Gz} \right)^{-0.545} \exp \left(\frac{-48.2}{Gz} \right) \quad (2.22)$$

$$Sh_H = 4.364 + 13.18 \left(\frac{1000}{Gz} \right)^{-0.524} \exp \left(\frac{-60.2}{Gz} \right) \quad (2.23)$$

Here Sh_T , Sh_H are Sherwood numbers at constant wall temperature and at constant wall heat flux respectively. Sherwood number is defined as

$$Sh = \frac{k_{i,m}L}{D_{i,A}} \quad (2.24)$$

Where $k_{i,m}$ is the convective mass transfer coefficient of species i , L is the characteristic length of the system (D_T for tubular reactor), $D_{i,A}$ is the diffusivity of the species i in the bulk of fluid A which is air. Graetz number is defined in the case of calculating convective mass transfer coefficient as

$$Gz = \frac{D_T}{z} ReSc \quad (2.25)$$

where Sc is the Schmidt number characteristic of hydrodynamic diffusivity relative with molecular diffusivity and is defined as

$$Sc = \frac{\mu}{\rho D_{i,A}} \quad (2.26)$$

where $D_{i,A}$ is the diffusivity of the species i in bulk A , here A is assumed to be air, which needs to be calculated based on the fluid temperature and pressure. In the system under study we are keeping the pressure constant along the reactor, so we need to find the diffusion coefficient based on the temperature of the fluid along the reactor.

2.4 Boundary Condition

Inlet boundary conditions $T_b=T_0$, $Y_i=Y_0$, $u=u_0$, $\rho=\rho_0$, $Y_{i,s}=0$ at $z=0$; Where T_b is the bulk temperature of the fluid, Y_i is the bulk mass fraction of species i , u is axial velocity, $Y_{i,s}$ is the surface concentration of the species i . Variables subscripted with 0 are their values at the inlet condition i.e. at $z=0$.

As combustion reactions are highly exothermic reactions, temperature in the system changes rapidly. So we cannot use constant transport property and thermodynamic property values such as viscosity, thermal conductivity of the fluid and specific heats of the species. Temperature and pressure dependencies are incorporated for calculating the transport and thermodynamic properties.

2.5 Transport Properties

2.5.1 Pure species viscosity and Binary diffusion coefficients

Pure component viscosity are given by the standard kinetic theory, the equation is[8]

$$\mu_k = \frac{5}{16} \frac{\sqrt{\pi m_k k_B T}}{\pi \sigma_k^2 \omega^{(2,2)*}} \quad (2.27)$$

Where m_k molecular weight, σ_k Lennard-Jones collision diameter, k_B Boltzmann constant, T temperature in K, $\omega^{(2,2)*}$ is the collision integral, depends on the reduced temperature given as

$$T_k^* = \frac{k_B T}{\epsilon_k} \quad (2.28)$$

and on reduced dipole moment given as

$$\delta_k^* = \frac{1}{2} \frac{\mu_k^2}{\epsilon_k \sigma_k^3} \quad (2.29)$$

ϵ_k is the Lennard-Jones potential well depth, μ_k is the dipole moment. The collision integral value is calculated using a quadratic interpolation of the tables of Stockmayer potentials given in Monchik and Mason[7]. Binary diffusion coefficients in terms of temperature and pressure is

$$D_{jk} = \frac{3}{16} \frac{\sqrt{2\pi k_B^3 T^3 / m_{jk}}}{P \pi \sigma_{jk}^2 \omega^{(1,1)*}} \quad (2.30)$$

where m_{jk} is the reduced molecular weight of species (j,k) pair given as

$$m_{jk} = \frac{m_j m_k}{m_j + m_k} \quad (2.31)$$

σ_{jk} is the reduced collision diameter, $\omega^{(1,1)*}$ is the collision integral based on Stockmayer potentials depends on reduced temperature T_{jk}^* , and reduced temperature depends on dipole moments μ_k and polarizabilities α_k . In the calculation of reduced quantities we consider two different cases such as both the colliding molecules are polar or non polar and one molecule is polar and the other is non polar. For the case of both the colliding molecules are polar or non polar expressions are as follows

$$\frac{\epsilon_{jk}}{k_B} = \sqrt{\frac{\epsilon_j \epsilon_k}{k_B^2}} \quad (2.32)$$

$$\sigma_{jk} = \frac{1}{2} (\sigma_j + \sigma_k) \quad (2.33)$$

$$\mu_{jk}^2 = \mu_j \mu_k \quad (2.34)$$

In the case of a polar molecule collision with non polar molecule and vice versa, the following expressions are used

$$\frac{\epsilon_{jk}}{k_B} = \zeta^2 \sqrt{\frac{\epsilon_j \epsilon_k}{k_B^2}} \quad (2.35)$$

$$\sigma_{jk} = \frac{1}{2} (\sigma_j + \sigma_k) \zeta^{-\frac{1}{6}} \quad (2.36)$$

$$\mu_{jk}^2 = 0 \quad (2.37)$$

Where

$$\zeta = 1 + \frac{1}{4} \alpha_p^* \mu_n^* \sqrt{\frac{\epsilon_p}{\epsilon_n}} \quad (2.38)$$

where α_p^* is the reduced polarization of non polar molecule and μ_p^* is the reduced dipole moment of polar molecule, these are given as

$$\alpha_n^* = \frac{\alpha_n}{\sigma_n^3} \quad (2.39)$$

$$\mu_p = \frac{\mu_p}{\sqrt{\epsilon_p \sigma_p^3}} \quad (2.40)$$

Evaluation of the collision integral $\omega^{(1,1)*}$ depends on the reduced temperature

$$T_{jk}^* = \frac{k_B T}{\epsilon_{jk}} \quad (2.41)$$

and the reduced dipole moment,

$$\delta_{jk}^* = \frac{1}{2} \mu_{jk}^{*2} \quad (2.42)$$

2.5.2 Pure species Thermal Conductivity

Pure species thermal conductivities are calculated using the following equations, we use them in finding the mixture thermal conductivity. These pure species conductivities are calculated based on translational, rotational, and vibrational contributions as described in Warnatz [9].

$$\lambda_k = \frac{\eta_k}{W_k} (f_{trans.} C_{v,trans.} + f_{rot.} C_{v,rot.} + f_{vib.} C_{v,vib.}) \quad (2.43)$$

where

$$f_{trans.} = \frac{5}{2} \left(1 - \frac{2}{\pi} \frac{C_{v,rot.}}{C_{v,trans.}} \frac{A}{B} \right) \quad (2.44)$$

$$f_{rot.} = \frac{\rho D_{kk}}{\eta_k} \left(1 + \frac{2}{\pi} \frac{A}{B} \right) \quad (2.45)$$

$$f_{vib} = \frac{\rho D_{kk}}{\eta_k} \quad (2.46)$$

and

$$A = \frac{5}{2} - \frac{\rho D_{kk}}{\eta_k} \quad (2.47)$$

$$B = Z_{rot} + \frac{2}{\pi} \left(\frac{5}{3} \frac{C_{v,rot.}}{R} + \rho D_{kk} \eta_k \right) \quad (2.48)$$

Depending on whether a molecule is linear or nonlinear heat capacity relationships will differ. For a linear molecule

$$\frac{C_{v,trans.}}{R} = \frac{3}{2} \quad (2.49)$$

$$\frac{C_{v,rot.}}{R} = 1 \quad (2.50)$$

$$C_{v,vib} = C_v - \frac{5}{2} R \quad (2.51)$$

Where C_v is the specific heat at constant volume of the molecule and R is the universal gas constant. For the case of nonlinear molecule the following relations hold,

$$\frac{C_{v,trans.}}{R} = \frac{3}{2} \quad (2.52)$$

$$\frac{C_{v,rot}}{R} = \frac{3}{2} \quad (2.53)$$

$$C_{v,vib.} = C_v - 3R \quad (2.54)$$

The translational part of C_v is always same. In the case of single atoms there will not be any internal contributions C_v and hence

$$\lambda_k = \frac{\eta_k}{W_k} \left(f_{trans.} \frac{3}{2} R \right) \quad (2.55)$$

where $f_{trans} = \frac{5}{2}$. Self diffusion coefficient D_{kk} is calculated as below

$$D_{kk} = \frac{3}{16} \frac{\sqrt{2\pi k_B^3 T^3 / m_k}}{P \pi \sigma_k^2 \omega^{(1,1)*}} \quad (2.56)$$

Density of the species is calculated by using the ideal gas law,

$$\rho = \frac{PW_k}{RT} \quad (2.57)$$

where p is the pressure and W_k is the species molecular weight.

The rotational relaxation collision number at 298 K is assumed. And its temperature dependence is calculated as follows[10] [11]

$$Z_{rot.}(T) = Z_{rot.}(298) \frac{F(298)}{F(T)} \quad (2.58)$$

where $F(T)$ is

$$F(T) = 1 + \frac{\pi^{\frac{3}{2}}}{2} \left(\frac{\epsilon/k_B}{T} \right)^{\frac{1}{2}} + \left(\frac{\pi^2}{4} + 2 \right) \left(\frac{\epsilon/k_B}{T} \right) + \pi^{\frac{3}{2}} \left(\frac{\epsilon/k_B}{T} \right)^{\frac{3}{2}} \quad (2.59)$$

2.5.3 Mixture Average Properties

Mixture properties are calculated by using the averaging formulas from the individual species properties as given below. The mixture average viscosity is given as

$$\eta = \sum_{k=1}^K \left(\frac{X_k \eta_k}{\sum_{j=1}^K X_j \Phi_{kj}} \right) \quad (2.60)$$

where Φ_{kj} is given by the following formula

$$\Phi_{kj} = \frac{1}{\sqrt{8}} \left(1 + \frac{W_k}{W_j}\right)^{-\frac{1}{2}} \left(1 + \left(\frac{\eta_k}{\eta_j}\right)^{\frac{1}{2}} \left(\frac{W_j}{W_k}\right)^{\frac{1}{4}}\right)^2 \quad (2.61)$$

Mixture average thermal conductivity is calculated using the averaging formula

$$\lambda = \frac{1}{2} \left(\sum_{k=1}^K X_k \lambda_k + \frac{1}{\sum_{k=1}^K K X_k / \lambda_k} \right) \quad (2.62)$$

Mixture Diffusion coefficient is calculated as

$$D_{km} = \frac{\sum_{j \neq k}^K X_j W_j}{\bar{W} \sum_{j \neq k}^K X_j / D_{jk}} \quad (2.63)$$

2.6 Thermodynamic Properties

Heat capacity at constant pressure, enthalpy and entropy values are very important in combustion systems which are useful in calculating other thermodynamic quantities such as heat of reaction, free energy change of reaction. Heat capacity at a constant pressure can be written as a polynomial of temperature. We are using NASA polynomials here, the expressions are as follows

$$\frac{C_{pk}^0}{R_g} = a_{1k} + a_{2k}T_k + a_{3k}T^2 + a_{4k}T^3 + a_{5k}T^4 \quad (2.64)$$

Enthalpy of a species is calculated as

$$H_k^0 = \int C_{pk}^0 dT \quad (2.65)$$

which on replacing C_{pk}^0 with the equation 3.7 results in the following form

$$\frac{H_k^0}{R_g T} = a_{1k} + \frac{a_{2k}}{2} T + \frac{a_{3k}}{3} T^2 + \frac{a_{4k}}{4} T^3 + \frac{a_{5k}}{5} T^4 + \frac{a_{6k}}{T} \quad (2.66)$$

Entropy of a species is calculated as

$$S_k^0 = \int \frac{C_{pk}^0}{T} dT \quad (2.67)$$

on replacing C_{pk}^0 with eq(3.7) we get

$$\frac{S_k^0}{R_g} = a_{1k} \ln T + a_{2k} T + \frac{a_{3k}}{2} T^2 + \frac{a_{4k}}{3} T^3 + \frac{a_{5k}}{4} T^4 + a_{7k} \quad (2.68)$$

Using these three properties we can calculate the other thermodynamic properties as follows. Heat capacity at constant volume is

$$C_{vk}^0 = C_{pk}^0 - R_g \quad (2.69)$$

Internal energy

$$U_k^0 = H_k^0 - R_g T \quad (2.70)$$

Gibb's free energy is

$$G_k^0 = H_k^0 - T S_k^0 \quad (2.71)$$

2.7 Mixture average properties

Average specific heat at constant pressure and at constant volume are

$$\bar{C}_p = \sum_{k=1}^K C_{pk} X_k \quad (2.72)$$

$$\bar{C}_v = \sum_{k=1}^K C_{vk} X_k \quad (2.73)$$

Mixture average enthalpy is

$$\bar{H} = \sum_{k=1}^K H_k X_k \quad (2.74)$$

Mixture average internal energy

$$\bar{U} = \sum_{k=1}^K U_k X_k \quad (2.75)$$

Before evaluating mixture average entropy we need to write the entropy of the species with the pressure and the mixing terms as

$$S_k = S_k^0 - R_g \ln X_k - R_g \ln(p/P_{atm}) \quad (2.76)$$

Now the other properties of the system like Gibb's free energy and Helmholtz energy are calculated using this new entropy equation. Gibb's free energy is

$$\bar{G} = \sum_{k=1}^K (H_k - T S_k) X_k \quad (2.77)$$

Helmholtz energy is

$$\bar{A} = \sum_{k=1}^K (U_k - T S_k) X_k \quad (2.78)$$

Chemical kinetics are very important in the combustion reactions. There are gas phase and surface reactions present in the catalytic combustion reactor, So both gas phase and surface reaction mechanisms are considered for calculating molar production rates of species at any point in the reactor.

2.8 Results and Discussions

Here a tubular reactor loaded with platinum is studied with two systems, one NO₂ decomposition, and another is methane total combustion in air. NO₂ decomposition is carried out in a reactor of length 10cm , radius of 7.5mm of uniform cross section, inlet velocity is 0.1m/s, inlet pressure is 1 atm ,with an inlet temperature of 600K and a wall temperature of 1073K. A composition of 6.3 percent by volume of NO₂ in a mixture of N₂ is combusted in a platinum loaded reactor with a surface site density of 2.720×10^{-9} mole/cm². The mechanism of NO₂ decomposition in presence of Pt as shown in Table.1 is used. Physical properties like transport properties and thermodynamic properties of the species are calculated according to the formulas described in the previous sections of the chapter, these formulas are incorporated in C++ library files known as CRATL. Governing equations of species balance, continuity equation and energy balance equations are solved using limex(Deuhardt et al., 1987) a differential algebraic equations(DAE) solver developed in Fortran which is a third party solver. A plot of Sherwood number with respect to length of the reactor is plotted. From the Fig.2.2 it is observed that the Sherwood number is high at inlet and it is decreased as the length reaches several millimeters, Sherwood number is an indication of the mass transfer coefficient in the reactor, hence it can be observed that the mass transfer coefficients of the species are high at the reactor inlet, it is because at that length boundary layer formation would have not started, but immediately after the entrance the Sherwood number is decreasing, an indication of formation of boundary layer and hence the resistance to mass transfer starts and hence lower mass transfer coefficients, which results in lower reaction rates. It is not the case if we model the reactions as PFR where the concentration is uniform across the cross section.

Table 2.1: Platinum mechanism for NO₂ decomposition

SNo	Reaction	A ^a	β ^a	E ^a
1.	O ₂ + 2Pt(s) → 2O(s)	7.00×10^{-2}	0.0	0.0
2.	NO + Pt(s) → NO(s)	8.50×10^{-1}	0.0	0.0
3.	NO ₂ + Pt(s) → NO ₂ (s)	9.00×10^{-1}	0.0	0.0
4.	O + Pt(s) → O(s)	1.00×10^{-0}	0.0	0.0
5.	2O(s) → O ₂ + Pt(s)	3.70×10^{21}	0.0	213.0
	The reaction rate is modified by an activated O(s) coverage i.e., $k = AT^\beta \exp(-E/RT) \exp(-\epsilon[H(s)]/RT)$ where activation parameter $\epsilon = 70\text{kJ/mol}$			
6.	NO(s) → NO + Pt(s)	1.00×10^{16}	0.0	90.0
7.	NO ₂ → NO ₂ + Pt(s)	1.00×10^{13}	0.0	60.0
8.	NO(s) + O(s) → NO ₂ (s) + Pt(s)	3.70×10^{21}	0.0	96.3
	The reaction is dependant on NO(s), and O(s) coverage, Activation parameter for NO(s) is 70kJ/mol and temperature exponent is 1, activation parameter for O(s) is 70kJ/mol			
9.	NO ₂ (s) → NO(s) + O(s)	3.70×10^{21}	0.0	79.57

^a Arrhenius parameters for the rate constants written in the form $k = A T^\beta \exp(-E/RT)$. The units of A are given in terms of moles, cubic meters, and seconds, E is the kJ/mol.

^b The surface coverage (e.g. [H(s)]) is specified as a site fraction .

^c Sticking coefficient. Total available site density for Pt is = 2.7×10^{-9} mol/cm²

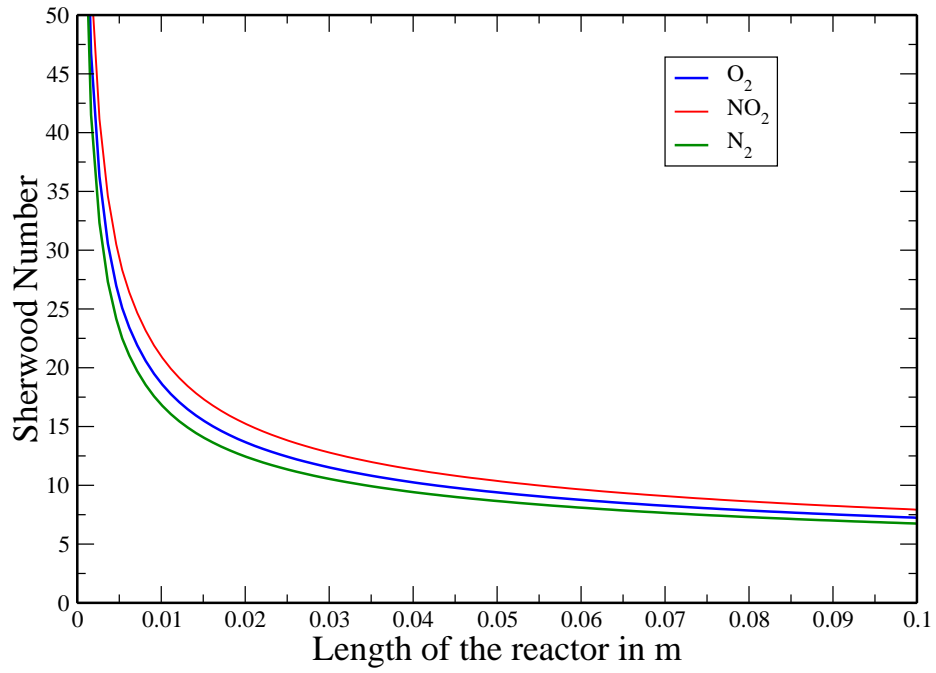


Figure 2.2: Sherwood number of the species NO_2 , NO , O_2 along with length of the reactor

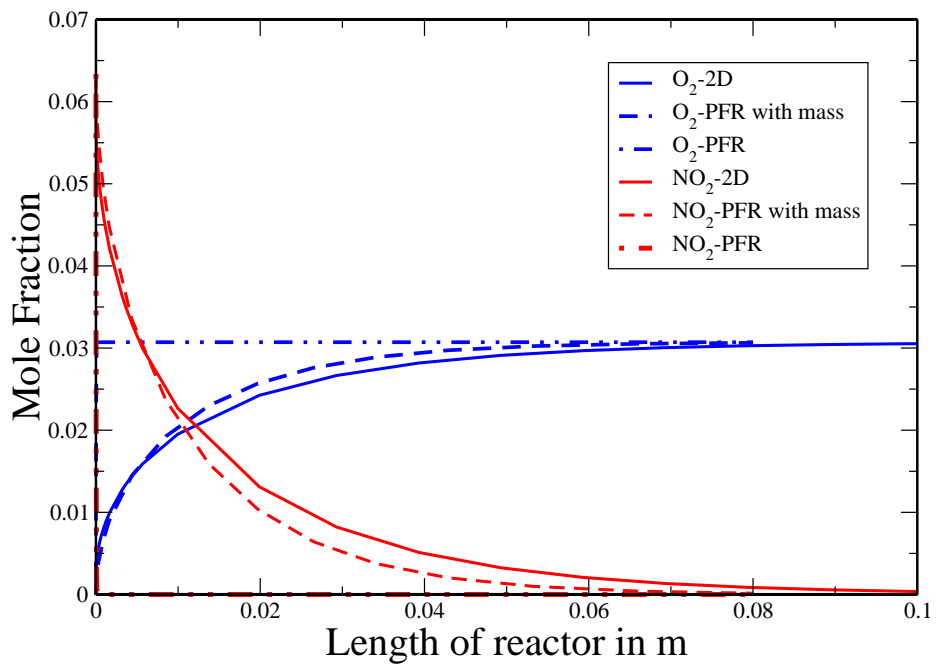


Figure 2.3: Mole fraction profiles of NO_2 and O_2 along the length for the three different models

A plot comparing the mole fractions of species NO_2 , O_2 is shown in the Fig.2.3. It can be observed that the concentration of NO_2 suddenly drops in the case of PFR, in the case of the 2D

model and PFR incorporated with mass transfer coefficients, the change in concentrations is slow and the difference is high, it is the result of the introduction of the mass transfer coefficients to calculate the concentrations at the surface. It emphasizes the importance of the correlations to find mass transfer coefficients. It can also be observed that the profiles for the PFR with mass transfer and 2D are close. This gives a motivation for developing more effective mass transfer correlations.

Another system which is total combustion of methane in presence of excess air and platinum catalyst is studied. The reactor is of length 5cm and 2mm diameter, the wall temperature is kept at 1290K(isothermal process), pressure at 1 atm. A 5% methane by volume in air mixture is considered for the combustion, velocity of the feed is 2 m/s, inlet temperature is 600K, and a surface density of $2.720 \times 10^{-9} \text{ mol/cm}^2$ is used. A Pt mechanism for total combustion of methane developed by Deutschmann [13] is described in the Table 2.2. Simulations are carried out with all the three models keeping all the conditions same and Sherwood number and mole fractions of the species along the reactor length are plotted.

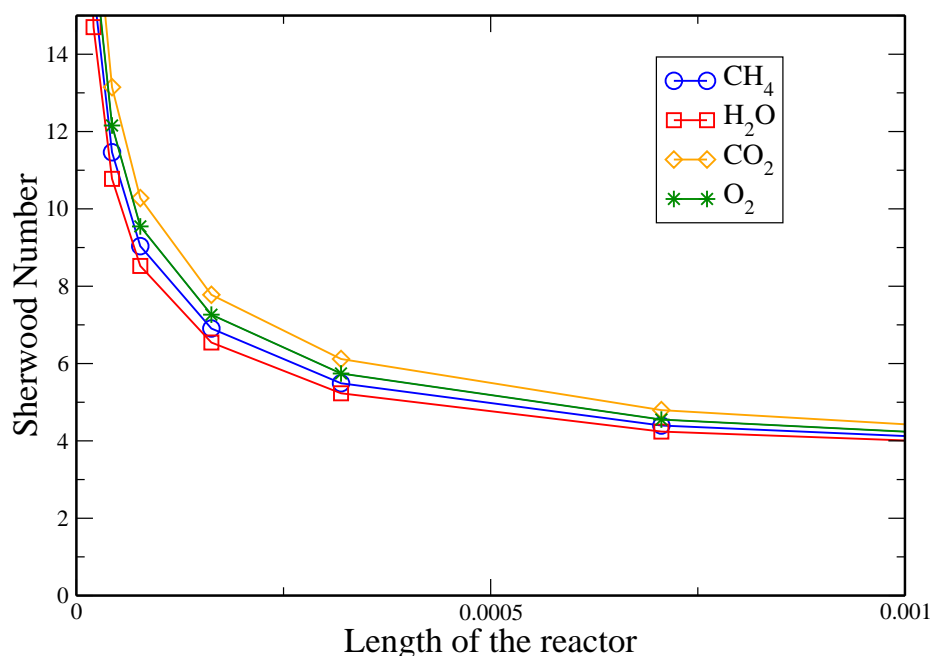


Figure 2.4: Sherwood number of the species CH₄, H₂O, CO₂ and O₂ along the length of reactor

From the Fig.2.4 we can observe the variation of Sherwood number with length for various species, the trend is similar to the previous case, but the Sherwood numbers for all the species are very close. At the entrance of the reactor Sherwood numbers are high as expected and they quickly decay as the length reaches several millimeters and by then the reaction will be in equilibrium and there will not be any concentration differences, that is why in all the models at the end the composition remains same corresponding to that temperature, pressure and inlet composition.

Table 2.2: Pt mechanism for methane combustion

SNo	Reaction	A^a	β^a	E^a
1.	$H_2 + 2Pt(s) \rightarrow 2H(s)$ The reaction rate is first order in Pt(s) The reaction is has an equivalent sticking coefficient of 0.046	4.46×10^{10}	0.5	
2.	$2H(s) \rightarrow H_2 + 2Pt(s)$ The reaction rate is modified by an activated H(s) coverage ^b i.e., $k = AT^\beta \exp(-\epsilon H(s)/RT)$ where activation parameter $\epsilon = -6\text{kJ/mol}$	3.70×10^{21}		67.3
3.	$H + Pt(s) \rightarrow H(s)$	1.00 ^c		
4.	$O_2 + 2Pt(s) \rightarrow 2O(s)$	1.80×10^{21}	-0.5	
5.	$O_2 + 2Pt(s) \rightarrow 2O(s)$ Reactions 4 and 5 represent alternative competing pathways	0.023 ^c		
6.	$2O(s) \rightarrow O_2 + 2Pt(s)$ The reaction rate is modified by an activates O(s) coverage, activation parameter is -60kJ/mol	1.8×10^{21}		213.2
7.	$O + Pt(s) \rightarrow O(s)$	1.0		
8.	$H_2O + Pt(s) \rightarrow H_2O(s)$	1.0		
9.	$H_2O(s) + Pt(s) \rightarrow H_2O + Pt(s)$	1.0×10^{13}		40.3
10.	$OH + Pt(s) \rightarrow OH(s)$	1.0		
11.	$OH(s) \rightarrow OH + Pt(s)$	1.0×10^{13}		192.8
12.	$H(s) + O(s) \rightarrow OH(s) + Pt(s)$	3.70×10^{21}		11.5
13.	$H(s) + OH(s) \rightarrow H_2O(s) + Pt(s)$	3.70×10^{21}		17.4
14.	$OH(s) + OH(s) \rightarrow H_2O + O(s)$	3.70×10^{21}		48.2
15.	$CO + Pt(s) \rightarrow CO(s)$ The reaction rate is 2nd order in Pt(s) The reaction is equivalent to a sticking coefficient of 0.84	1.618×10^{20}	0.5	
16.	$CO(s) \rightarrow CO + Pt(s)$	1.0×10^{13}		125.5
17.	$CO_2(s) \rightarrow CO_2 + Pt(s)$	1.0×10^{13}	20.5	
18.	$CO(s) + O(s) \rightarrow CO_2 + Pt(s)$	3.70×10^{21}		105.0
19.	$CH_4 + 2Pt(s) \rightarrow CH_3(s) + H(s)$ The reaction rate has a 2.3 order dependance on Pt(s) The reaction is equivalent to a sticking coefficient of 0.01	4.63×10^{20}	0.5	
20.	$CH_3(s) + Pt(s) \rightarrow CH_2(s) + H(s)$	3.7×10^{21}		20.0
21.	$CH_2(s) + Pt(s) \rightarrow CH(s) + H(s)$	3.7×10^{21}		20
22.	$CH(s) + Pt(s) \rightarrow C(s) + H(s)$	3.7×10^{21}		20
23.	$C(s) + O(s) \rightarrow CO(s) + Pt(s)$	3.7×10^{21}		62.8
24.	$CO(s) \rightarrow C(s) + O(s)$	1.0×10^{18}		184.0

^aArrhenius parameters for the rate constants written in the form $k = A T^\beta \exp(-E/RT)$. The units of A are given in terms of moles, cubic meters, and seconds, E is the kJ/mol.

^b The surface coverage (e.g. [H(s)]) is specified as a site fraction .

^c Sticking coefficient. Total available site density for Pt is $= 2.7 \times 10^{-9}$ mol/cm²

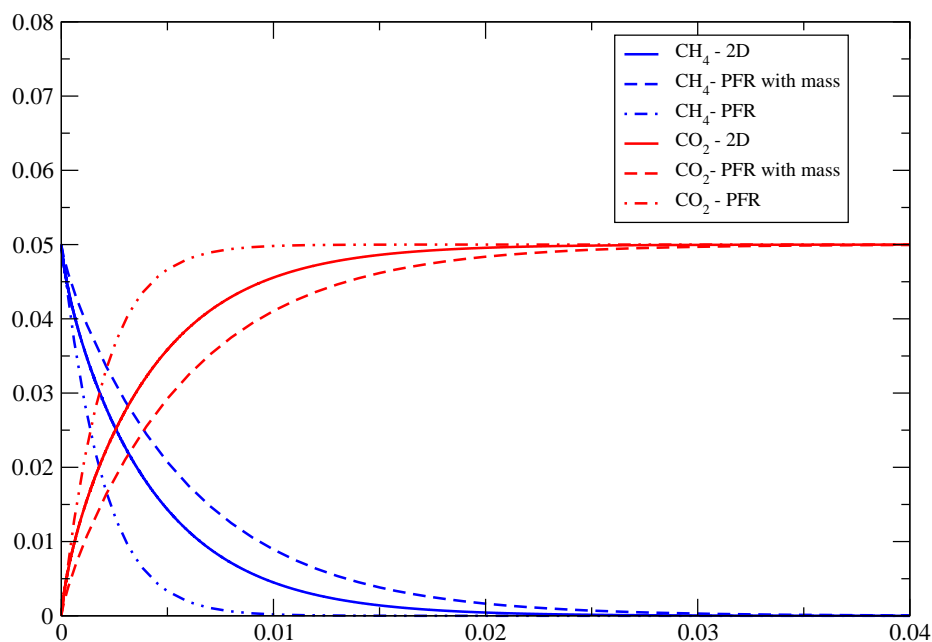


Figure 2.5: Mole fraction profiles of species CH₄, H₂O, CO₂, O₂ when methane combusted with Pt catalyst

2.9 Summary

From the two systems studied above it is clear that plug flow modeling will predict a poor composition profile in a tubular reactor when compared to 2D model. A plug flow model with mass transfer limitation modeled using a mass transfer correlation gives comparable results with that of 2D boundary layer model. When accurate results are not necessary we can use plug flow with mass transfer limitation, which reduces the time required for simulation, which will complete in a several minutes.

Chapter 3

Equilibrium Composition Calculations

3.1 Formulation

Here a procedure is described to calculate the equilibrium composition which is adapted from Milo D. Koretsky's book on thermodynamics "Engineering and Chemical Thermodynamics". Equilibrium composition code is developed to check the final compositions or the equilibrium compositions obtained using the channel reactors that we are simulating in the current study by implementing the mass transfer and heat transfer limitations. It also helps in validation of the reaction mechanism adapted in a certain temperature range. Some reaction mechanisms may not be valid in certain temperature range, In such a case to validate the temperature range for a particular mechanism this equilibrium code can be used. It is based on the principles that the total number of the atoms present in the system at any point will be same[6].

Generalized method for finding the equilibrium composition can be described as follows. Assuming there are m number of species present in the system at equilibrium, k is the number of the different atoms whose combination in several ways can make up the system during the reactions, and n_i is the number of moles or mole fraction of the species i (i can have a value 0 to $m - 1$) in the system. A relation between the number of moles of the species and the elements present in each species with the total number of elements in the system can be written as follows,

$$A_{k \times m} X_{m \times 1} = B_{k \times 1} \quad (3.1)$$

Where the matrix A in the row wise gives the number of elements present in each species of the system in each column, likewise it gives for all the species in the system. So each row gives for a particular element in the system. X is a column matrix which gives the number of moles of each species in the system, B gives the total number of moles of species in the system which depend on the input composition of the system. Both Matrices A and B are unchanged in the system until we change the initial composition or the number of species present in the system. X varies with the temperature. Relation given by Eq.(3.1) gives k equations in terms of the number of moles of the species.

If we consider n_i as the number of moles of the species i in the system, $a_{i,j}$ is used to represent the elements of the matrix A , and b_i represent the elements of the matrix B , Then the k equations are given as

$$\sum_{j=1}^{j=m} a_{i,j} n_j = b_i \quad (3.2)$$

Where i varies from $i = 1$ to $i = k$ i.e one equation for balance of moles of one element from all the species in the system, there will be k such equations. Using the minimization of Gibb's free energy m equations can be formed as

$$\Delta g_{f,l}^0 + RT \ln \frac{n_l}{n_T} + \lambda_i a_{i,l} = 0 \quad (3.3)$$

Here $\Delta g_{f,l}^0$ is the Gibb's free energy of species l at the given temperature and pressure, n_l is number of moles of species l . Gibbs energy of species is calculated by using the thermodynamic formulas available in the C++ library which implements all the thermodynamic and transport properties according to the principles discussed in the chapter 2. We have $m + k$ equations here and $m + k$ variables. These equations constitute a nonlinear system of equations. A C++ code is developed and added to the software CRMS developed by Dr. Vinod M. Janardhanan to read the number of species, their initial mole fractions, reaction temperature and to form the A, B matrices. The resulting equations are solved using Newton Solver.

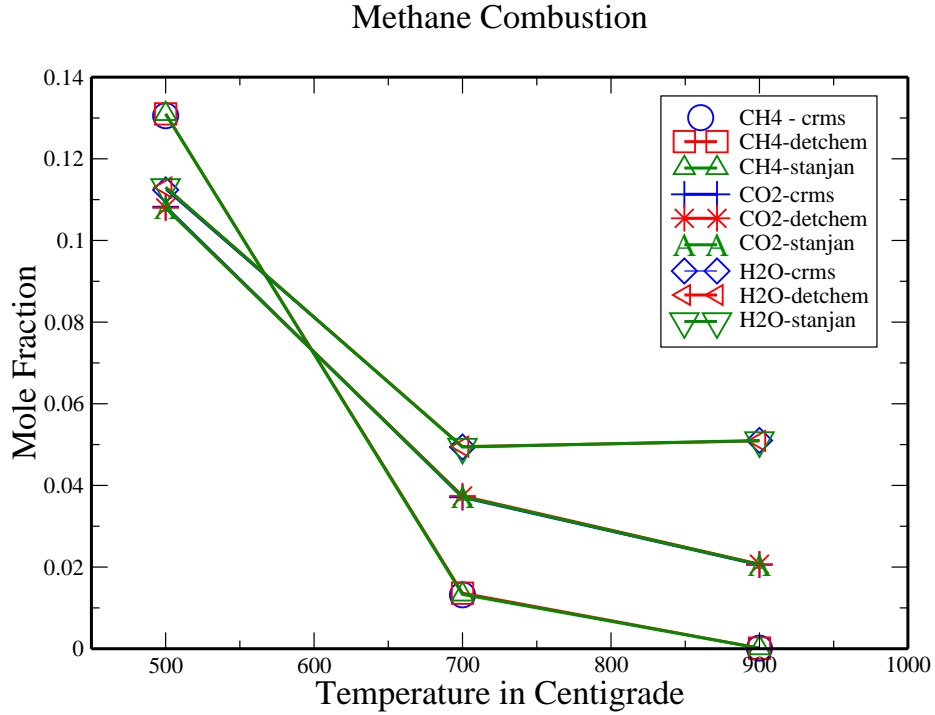


Figure 3.1: Comparison of the compositions obtained from various Softwares, for methane partial combustion

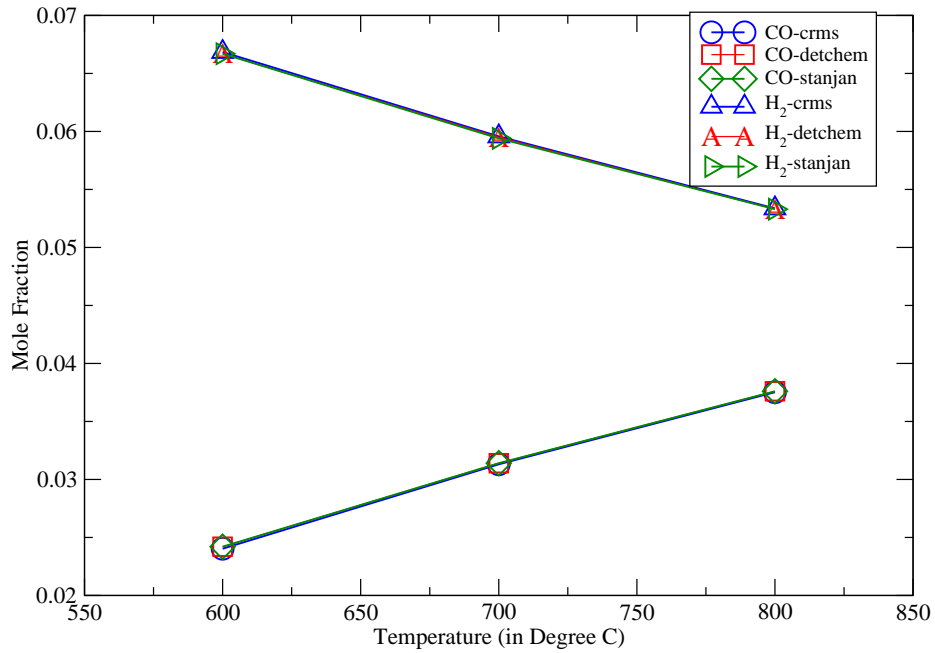


Figure 3.2: Comparison of the compositions obtained from various Softwares, for Propane partial combustion

3.2 Results and Validation

The results obtained using our code is thoroughly validated with the other available softwares like DETCHEM, GASEQ, STANJAN which are some widely used softwares in the scientific community. Two systems are analyzed for equilibrium compositions in three different codes, including our code, one is 3:4 ratio of methane to oxygen system, which falls nearly in total combustion range and a temperature range of 600⁰ to 1000⁰C. Another system is a 5 percent propane in air, which falls in the partial combustion composition is analyzed at different temperatures ranging from 600⁰C to 1000⁰C. For the above two cases mole fractions are plotted for key species like methane, propane, CO and H₂, CO₂, H₂O in Fig.3.1 and Fig.3.2.

Fig.3.1 shows equilibrium mole fraction of CH₄, CO₂, H₂O when methane of same inlet mole fraction is used at different temperatures, it can be clearly observed that the three cases are merging each other, giving the same equilibrium composition for all the softwares. Fig.3.2 shows equilibrium mole fractions when propane is reacted with air, here oxygen is used less, so that partial combustion occurs to form H₂, CO components as major products. It is clear from the figure that all the equilibrium compositions at different temperatures for different softwares have same values and the lines are indistinguishable.

3.3 Summary

Equilibrium composition code developed is in very good agreement with the any other good package available. It can be used to any system of components given the thermodynamic data files in the NASA polynomial format.

Chapter 4

Mechanism Validation

4.1 Background

A detailed mechanism developed based on experiments under certain conditions of physical parameters is valid only to those conditions under which it is developed, but people use mechanisms out of the range in which it is supposed to be used. This study of comparison of the maximum possible conversion with the equilibrium conversion for certain range of temperature, pressure and concentration ratios in terms of equivalent ratio may give us some insight into the mechanism validity.

Plug flow reactor of certain radius and a length such that the system comes to equilibrium by the time the reactants and products reaches the other end (Length of 20cm is used). Rhodium mechanism for the partial combustion of methane is assessed. Pressure is kept constant at 1 atm for all the simulations, temperature is varied from 500⁰C to 1200⁰C, equivalence ratio varies from 0.25 to approximately 10. Equivalence ratio is 1 when CH₄ to O₂ ratio is 2:1 which is for complete partial combustion situation, equivalence ratio equal to or more than 1 is corresponding to partial combustion of methane.

The concentrations of the various species at the exit of the reactor is compared with the concentrations of various species calculated using equilibrium code. Conversion obtained by any reactor developed should be lower than the conversion obtained by equilibrium. The comparison of concentration for various temperatures are plotted below.

It is observed from the results that the mechanism is not appropriate at certain equivalence ratios, this also changes with temperature. And the mechanism is giving good results for the values of equivalence ratios of 1 or more than 1. It is also observed from the graphs that the mole fractions of water and carbon dioxide are more than what equilibrium predicts, so it requires the mechanism to be refined yet with respect to H₂O and CO₂. From this analysis we can say that any published mechanism cannot be used beyond certain range of values for composition and at a particular temperature.

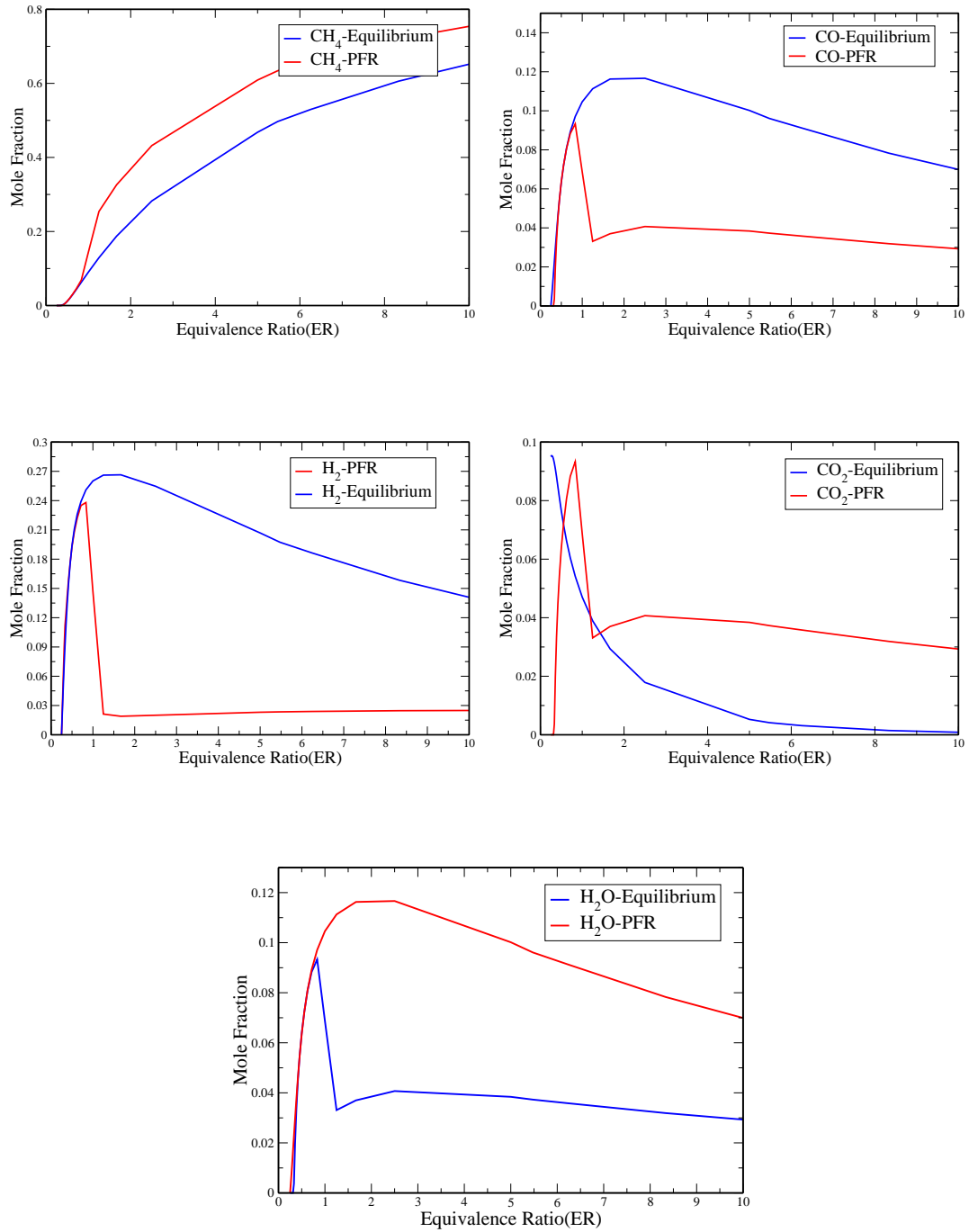


Figure 4.1: Comparison of the PFR compositions and equilibrium compositions at 600⁰ C

4.2 Results and Discussions

Here methane partial combustion mechanism with Rhodium is analyzed for its validity in the wide range of Equivalence ratio and at different temperatures. Detailed surface reaction mechanism developed by Deutschmann et al 2001[12], presented in Table 4.1. Plug flow reactor is used to

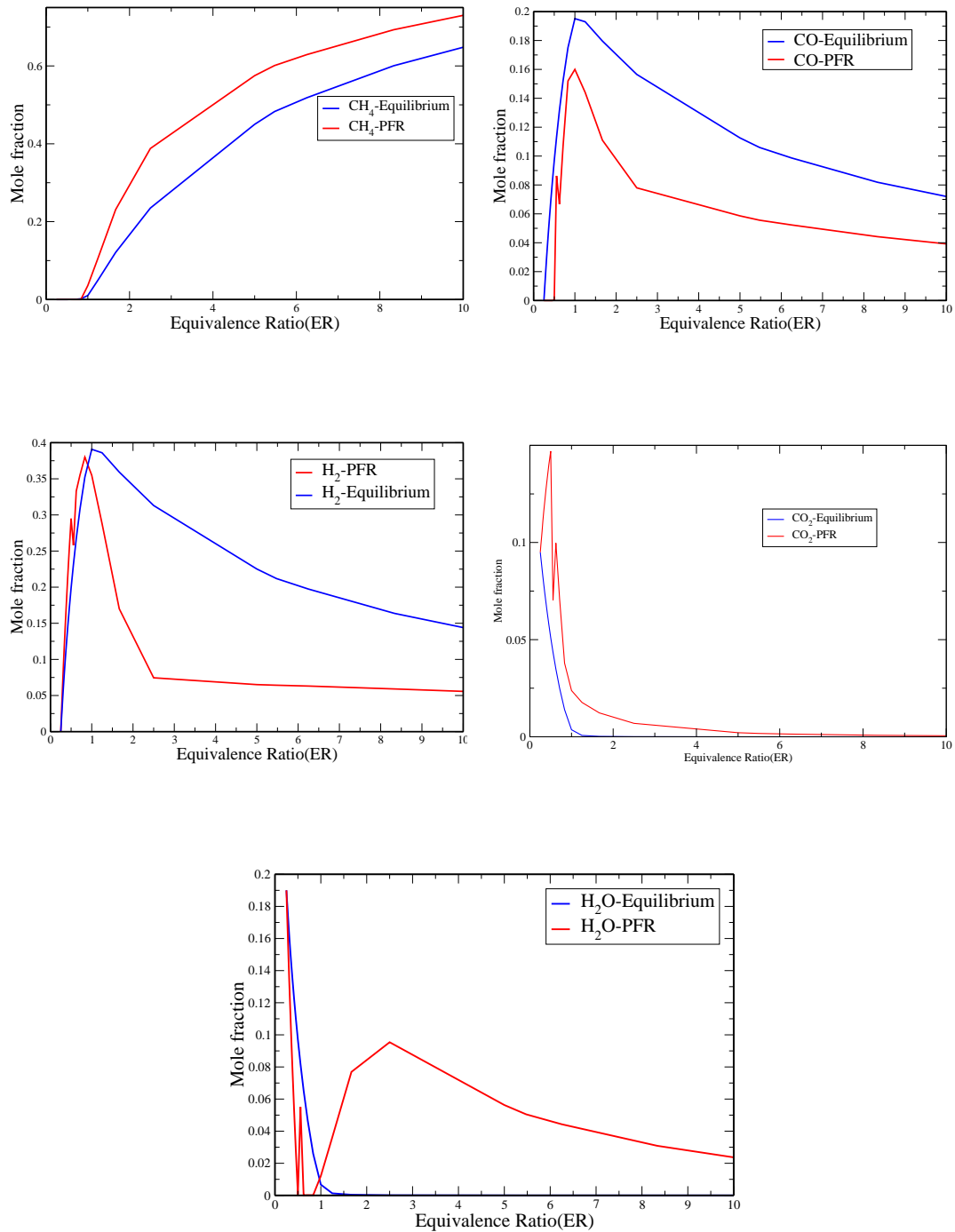


Figure 4.2: Comparison of the PFR compositions and equilibrium compositions at 800°C

simulate the methane partial combustion to obtain the equilibrium composition from the model for the Rhodium mechanism. Equivalence ratio of 0.25 to 10 is used to simulate the combustion in the temperature range of 600°C to 1000°C with an interval of 100°C . Velocity is not a constraint here as the length of the reactor is taken long enough to equilibrate the reactants. But a reactor length

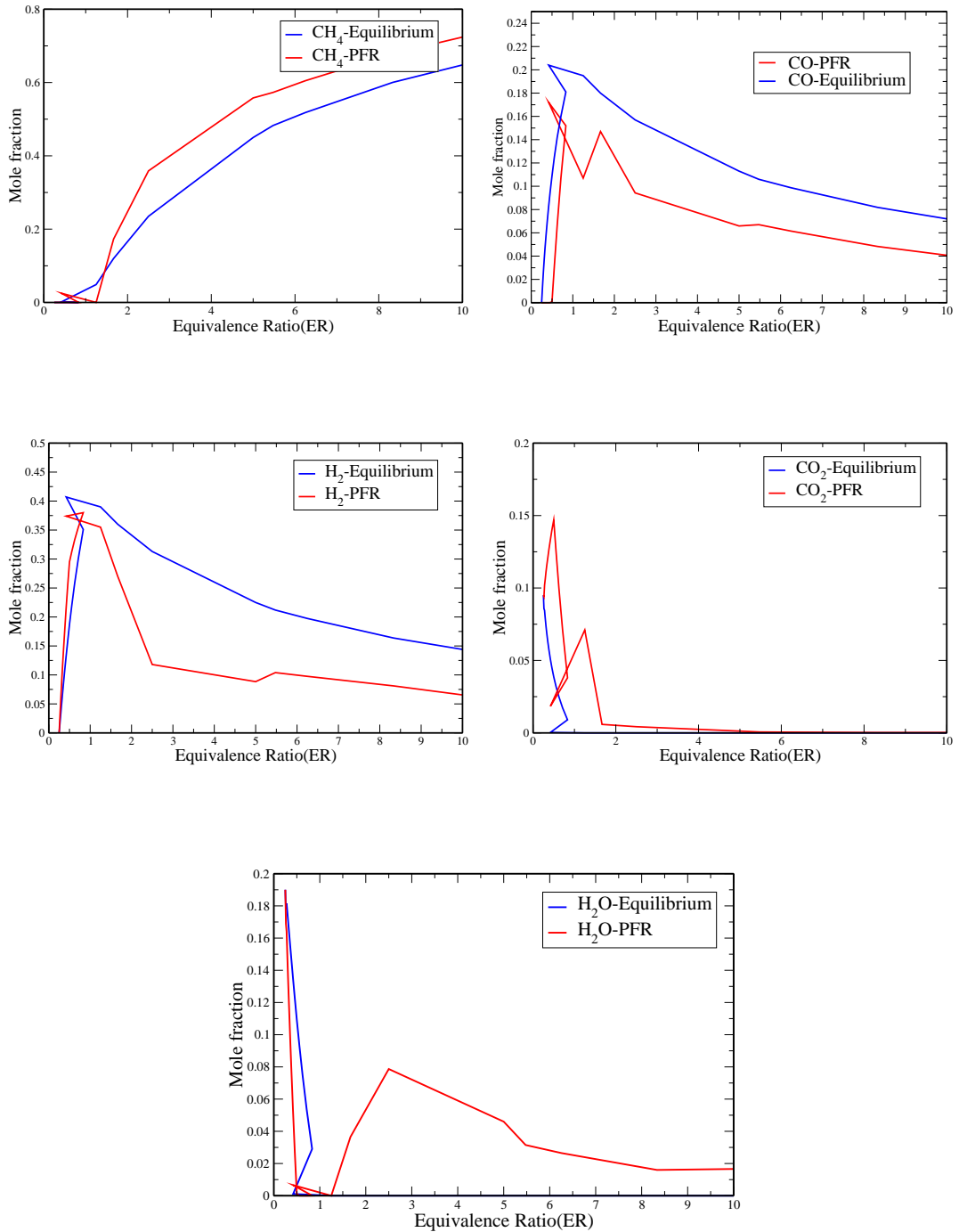


Figure 4.3: Comparison of the PFR compositions and equilibrium compositions at 1000⁰C

of 20cm is almost long enough to reach equilibrium. Pressure is maintained at 1atm, radius of the reactor is 1mm. For each equivalence ratio and temperature equilibrium compositions from both PFR model and from Equilibrium code are noted for the comparison. Similar procedure is carried out till Equivalence ratio reaches 10. The intermediate points are chosen such a way that around 10 to 15 points are available. The species profiles at three temperatures 600⁰C, 800⁰C, 1000⁰C are shown here.

Table 4.1: Rh mechanism for Methane partial combustion

SNo	Reaction	A^a	β^a	E^a
1.	$\text{H}_2 + 2\text{Rh(s)} \rightarrow 2\text{H(s)}$	0.01	0.0	0.0
2.	$\text{O}_2 + 2 \text{Rh(s)} \rightarrow 2\text{O(s)}$	0.01	0.0	0.0
3.	$\text{CH}_4 + \text{Rh(s)} \rightarrow \text{CH}_4\text{(s)}$	8.0×10^{-3}	0.0	0.0
4.	$\text{H}_2\text{O} + \text{Rh(s)} \rightarrow \text{H}_2\text{O(s)}$	1.0×10^{-1}	0.0	0.0
5.	$\text{CO}_2 + \text{Rh(s)} \rightarrow \text{CO}_2\text{(s)}$	1.0×10^{-5}	0.0	0.0
6.	$\text{CO} + \text{Rh(s)} \rightarrow \text{CO(s)}$	5.01×10^{-1}	0.0	0.0
7.	$2\text{H(s)} \rightarrow \text{H}_2 + 2\text{Rh(s)}$	3.0×10^{21}	0.0	77.8
8.	$2\text{O(s)} \rightarrow \text{O}_2 + 2\text{Rh(s)}$	1.30×10^{22}	0.0	355.2
9.	$\text{H}_2\text{O(s)} \rightarrow \text{H}_2\text{O} + \text{Rh(s)}$	3.0×10^{13}	0.0	45
10.	$\text{CO(s)} \rightarrow \text{CO} + \text{Rh(s)}$	3.50×10^{13}	0.0	133.4
11.	$\text{CO}_2\text{(s)} \rightarrow \text{CO}_2 + \text{Rh(s)}$	1.0×10^{13}	0.0	21.7
12.	$\text{CH}_4\text{(s)} \rightarrow \text{CH}_4 + \text{Rh(s)}$	1.0×10^{13}	0.0	25.1
13.	$\text{H(s)} + \text{O(s)} \rightarrow \text{OH(s)} + \text{Rh(s)}$	5.0×10^{22}	0.0	83.7
14.	$\text{OH(s)} + \text{Rh(s)} \rightarrow \text{O(s)} + \text{H(s)}$	3.0×10^{20}	0.0	37.7
15.	$\text{H(s)} + \text{OH(s)} \rightarrow \text{H}_2\text{O(s)} + \text{Rh(s)}$	3.0×10^{20}	0.0	33.5
16.	$\text{H}_2\text{O(s)} + \text{Rh(s)} \rightarrow \text{H(s)} + \text{OH(s)}$	5.0×10^{22}	0.0	106.4
17.	$\text{OH(s)} + \text{OH(s)} \rightarrow \text{H}_2\text{O(s)} + \text{O(s)}$	3.0×10^{21}	0.0	100.8
18.	$\text{H}_2\text{O(s)} + \text{O(s)} \rightarrow \text{OH(s)} + \text{OH(s)}$	3.0×10^{21}	0.0	224.2
19.	$\text{C(s)} + \text{O(s)} \rightarrow \text{CO(s)} + \text{Rh(s)}$	3.0×10^{22}	0.0	97.9
20.	$\text{CO(s)} + \text{Rh(s)} \rightarrow \text{C(s)} + \text{O(s)}$	2.5×10^{21}	0.0	169.0
21.	$\text{CO(s)} + \text{O(s)} \rightarrow \text{CO}_2\text{(s)} + \text{Rh(s)}$	1.4×10^{20}	0.0	121.6
22.	$\text{CO}_2\text{(s)} + \text{Rh(s)} \rightarrow \text{CO(s)} + \text{O(s)}$	3.0×10^{21}	0.0	115.3
23.	$\text{CH}_4\text{(s)} + \text{Rh(s)} \rightarrow \text{CH}_3\text{(s)} + \text{H(s)}$	3.70×10^{21}	0.0	61.0
24.	$\text{CH}_3\text{(s)} + \text{H(s)} \rightarrow \text{CH}_4\text{(s)} + \text{Rh(s)}$	3.7×10^{21}	0.0	51.0
25.	$\text{CH}_3\text{(s)} + \text{Rh(s)} \rightarrow \text{CH}_2\text{(s)} + \text{H(s)}$	3.7×10^{24}	0.0	103.0
26.	$\text{CH}_2\text{(s)} + \text{H(s)} \rightarrow \text{CH}_3\text{(s)} + \text{Rh(s)}$	3.7×10^{21}	0.0	44.0
27.	$\text{CH}_2\text{(s)} + \text{Rh(s)} \rightarrow \text{CH(s)} + \text{H(s)}$	3.7×10^{24}	0.0	100.0
28.	$\text{CH(s)} + \text{H(s)} \rightarrow \text{CH}_2\text{(s)} + \text{Rh(s)}$	3.7×10^{21}	0.0	68.0
29.	$\text{CH(s)} + \text{Rh(s)} \rightarrow \text{C(s)} + \text{H(s)}$	3.7×10^{21}	0.0	21.0
30.	$\text{C(s)} + \text{H(s)} \rightarrow \text{CH(s)} + \text{Rh(s)}$	3.7×10^{21}	0.0	172.8
31.	$\text{CH}_4\text{(s)} + \text{O(s)} \rightarrow \text{CH}_3\text{(s)} + \text{OH(s)}$	1.7×10^{24}	0.0	80.3
32.	$\text{CH}_3\text{(s)} + \text{OH(s)} \rightarrow \text{CH}_4\text{(s)} + \text{O(s)}$	3.7×10^{21}	0.0	24.3
33.	$\text{CH}_3\text{(s)} + \text{O(s)} \rightarrow \text{CH}_2\text{(s)} + \text{OH(s)}$	3.7×10^{24}	0.0	120.3
34.	$\text{CH}_2\text{(s)} + \text{OH(s)} \rightarrow \text{CH}_3\text{(s)} + \text{O(s)}$	3.7×10^{21}	0.0	15.1
35.	$\text{CH}_2\text{(s)} + \text{O(s)} \rightarrow \text{CH(s)} + \text{OH(s)}$	3.7×10^{24}	0.0	158.4
36.	$\text{CH(s)} + \text{OH(s)} \rightarrow \text{CH}_2\text{(s)} + \text{O(s)}$	3.7×10^{21}	0.0	36.8
37.	$\text{CH(s)} + \text{O(s)} \rightarrow \text{C(s)} + \text{OH(s)}$	3.7×10^{21}	0.0	30.1
38.	$\text{C(s)} + \text{OH(s)} \rightarrow \text{CH(s)} + \text{O(s)}$	3.7×10^{21}	0.0	145.5

^a Arrhenius parameters for the rate constants written in the form $k=A T^\beta \exp(-E/RT)$. The units of A are given in terms of moles, cubic meters, and seconds, E is the kJ/mol.

^b The surface coverage (e.g. $[\text{H(s)}]$) is specified as a site fraction.

^c Sticking coefficient. Total available site density for Pt is $= 2.7 \times 10^{-9}$ mol/cm²

From Figs. 4.1 to 4.3 the temperature dependence is not much observed, so it is the fuel to air ratio, or Equivalence ratio whichever requires attention in using it for our applications. Coming to the effect of equivalence ratio on the outlet composition, from the figure 4.1 the composition of CH₄, CO, H₂ are considerable as they are below the equilibrium limits for equivalence ratio of 1 and more than one, any reaction cannot go beyond the equilibrium composition. From the figures it can be observed that the methane mole fraction is more than that of equilibrium which means that the conversion of PFR model is less than equilibrium predicts, which is valid observation as any real reaction cannot go beyond the equilibrium conversion. Similarly on observing the mole fractions of H₂, CO which are the products of partial combustion of methane, PFR gives lower mole fractions than that of equilibrium compositions, which is expected. It can also be observed that the mole fractions of components H₂O, CO₂ are more than that equilibrium compositions. Species H₂O and CO₂ will also present in products of methane partial combustion, product cannot be more than that what equilibrium predicts.

4.3 Summary

As methane conversion, and the formation of the major products are in good agreement with equilibrium mole fractions for values of equivalent ratio greater than 1, for which the mechanism is developed for, it should be strictly used in this range of equivalence ratio to give reliable compositions. And also the mechanism requires more refinement with respect to formation of water and carbon dioxide molecules.

Chapter 5

Summary

We have studied behavior of tubular reactors under different ways of modeling, namely plug flow reactor, plug flow with mass transfer limitation and modeling in 2 Dimensions. We have compared the results in all the three cases, and differences exists for all, but the difference of plug flow reactor results are high and we can come to a conclusion that plug flow reactor cannot be used for combustion processes, where as the differences for plug flow with mass transfer and 2 model are low, so that we can use plug flow model with mass transfer in place of 2D model to reduce time consumption with nearly same results. This also emphasizes importance of the widely valid mass transfer correlations to predict accurate reaction rates and concentrations on the surface of the catalysts. A C++ code for calculating the equilibrium composition is developed and is validated with other available codes. A mechanism validating study is carried out, where the exit compositions of the plug flow reactor using the Rhodium mechanism for methane partial combustion for different equivalence ratios and different temperatures. The results are compared with the results obtained from the equilibrium code. The results showed that for some of the species the compositions are comparable with equilibrium compositions for the values of equivalence ratio 1 and above, but still for some species ,i.e for H_2O , CO_2 are erroneous, which emphasizes that the mechanism may have to be refined to give good results for the species mentioned. In future we can use more efficient mass transfer correlations and using this the differences for 2D and PFR with mass transfer model can be even reduced, which can save time to simulate such processes with tubular reactors.

References

- [1] R.E. Hayes, S.T. Kolaczkowski. Introduction To Catalytic Combustion. *Gordan and Breach science Publishers*, (1997)
- [2] Vesna Tomasic, Franjo Jovic. State-of-the-art in the monolithic catalysts or reactors. *Appl. Catal. A* 311,(2006) (112-121)
- [3] Jan Kaspar, Paolo Fornasiero, Neal Hickey. Automotive catalytic converters: current status and some perspectives. *Catal. Today*77, (2003) (419-449)
- [4] Laxminarayan L. Raja, Robert J. Kee, Olaf Deutschmann, Juergen Warnatz, Lanny D. Schmidt. A critical evaluation of NavierStokes, boundary-layer, and plug-flow models of the flow and chemistry in a catalytic-combustion monolith . *Catal. Today*59, (2000) (47-60)
- [5] Renate Schwiedernoch, Ste en Tischer, Chrys Correa, . Experimental and numerical study on the transient behavior of partial oxidation of methane in a catalytic monolith. *Chem. Eng. Sci.* 58, (2003)(633-642)
- [6] Milo D. Koretsky. Engineering and Chemical Thermodynamics. *John Wiley & Sons (Asia) pte Ltd.*, (2004)
- [7] L. Monchick, E. A. Mason. Transport properties of polar gases. *J. Chem. Phys.* 35, (1961) (1676).
- [8] J. O. Hirschfelder, C. F. Curtiss, R. B. Bird. Molecular Theory of Gases and Liquids. *John Wiley and Sons, New York.*, (1954)
- [9] N. Peters, J. Warnatz. Numerical Methods in Flame Propagation. *Vieweg*, (1982)
- [10] J. G. Parker. Rotational and Vibrational Relaxation in Diatomic Gases. *Phys. Fluids*, (1959)
- [11] C. C. Brau, R. M. Jonkman. Classical theory of rotational relaxation in diatomic gases. *J. Chem. Phys.*, (1970)
- [12] Deutschmann, O., Correa, C., Tischer, S., Chatterjee, D., Kleditzsch, S., Warnatz, J.. Natural gas conversion in Monolithic Catalysts: Interaction of Chemical reactions and Transport phenomena. *Stud. Surf. Sci. Catal.*, (2001)
- [13] Olaf Deutschmann, Frank Behrendt, Jrgen Warnatz. Formal Treatment of Catalytic Combustion and Catalytic Conversion of Methane. *Catal. Today* 46, (1998) (155-163)